NASA TECHNICAL NOTE

NASA TN D-4303

SPECTRAL EMISSIVITY OF HIGHLY DOPED SILICON

by Curt H. Liebert and Ralph D. Thomas

Lewis Research Center
Cleveland, Ohio

NATIONAL AERONAUTICS AND SPACE ADMINISTRATION • WASHINGTON, D. C. • APRIL 1968

SPECTRAL EMISSIVITY OF HIGHLY DOPED SILICON

By Curt H. Liebert and Ralph D. Thomas

Lewis Research Center
Cleveland, Ohio

NATIONAL AERONAUTICS AND SPACE ADMINISTRATION

For sale by the Clearinghouse for Federal Scientific and Technical Information
Springfield, Virginia 22151 – CFSTI price $3.00

SPECTRAL EMISSIVITY OF HIGHLY DOPED SILICON*

by Curt H. Liebert and Ralph D. Thomas

Lewis Research Center

SUMMARY

Measurements were made at temperatures of 300°, 882°, and 1074° K of the normal spectral emissivity of opaque, highly doped silicon. The silicon was doped with arsenic and boron to electron carrier concentrations of 2.2×10^{19}, 3.7×10^{19}, and 8.5×10^{19} electrons per cubic centimeter and hole carrier concentrations of 6.2×10^{19} and 1.4×10^{20} holes per cubic centimeter. The 300° K emissivity data were obtained at wavelengths from 2.5 to 35 microns. The high temperature emissivities were measured from 3.5 to 14.8 microns.

Carrier concentrations and direct-current resistivity of the silicon were also measured. The carrier concentrations were determined from Hall measurements made at 300° K. The direct-current resistivity was measured at temperatures from 300° to 1200° K. These quantities (among others) were used in analytical calculations of the emissivities.

Agreement of the Hagan-Rubens theory with experiment was found at wavelengths greater than 12 microns and at 300° K. Good agreement of the free carrier absorption theory with experiment was achieved at all wavelengths and temperatures investigated.

The free carrier absorption theory predicts the emissivity in terms of the index of refraction and the absorption index. The values of these quantities are presented. A comparison of the values of the absorption index obtained herein with those obtained from the literature showed good qualitative agreement.

INTRODUCTION

There is considerable theory relating emissivity, absorptivity, transmissivity, and reflectivity to the composition of homogeneous materials. Therefore, a better understanding of the optical properties of homogeneous materials could lead to a more com-

*Published in Thermophysics of Spacecraft and Planetary Bodies, vol. 20 of AIAA series Progress in Astronautics and Aeronautics, Gerhard B. Heller, ed., Academic Press, 1967, pp. 17-40.

plete insight of the properties required for radiant heat-transfer calculations with a variety of materials. While a quantitative description of the latter may never be achieved, a fundamental understanding of the optical properties of a material may permit extrapolation of measured data to temperatures or wavelengths beyond the convenient experimental range.

In recent years, many theoretical attempts have been made to explain the phenomenon of dispersion by relating the optical properties of smooth, homogeneous metals, dielectrics, and semiconductors to electrical properties. Two approaches are the Hagan-Rubens theory (hereinafter called HR) (ref. 1) and the metallic or free carrier absorption theory (hereinafter called FCA) (ref. 2).

The HR theory is based on an idealized physical model and leads to a simple expression for the normal spectral emissivity in terms of the wavelength and the direct current resistivity. This theory is known to work well for metals at near room temperature and at wavelengths greater than about 10 microns. However, no investigations have been made in which this theory was applied to highly doped semiconductors.

The FCA theory is more general, and the resulting equations for emissivity are necessarily more complex. This theory agrees well with the experimental optical properties of metals at wavelengths longer than 0.75 microns and over a wide range of temperature. Good agreement has also been found between this theory and the optical properties of dielectrics when measured over a wide temperature range. Also, the FCA theory predicts well the room-temperature emissivity of semiconductors. However, this theory has not been applied to the spectral emissivity of semiconductors at elevated temperatures.

In this investigation, the normal spectral emissivities of highly doped, single crystal, n- and p-type silicon with optically smooth surfaces were determined experimentally in air at 300°, 882°, and 1074° K. Calculated emissivities as predicted by the HR and the FCA theories were then compared with the experimental results.

The variation of direct-current resistivity with temperature and the room-temperature Hall coefficient also were determined experimentally. The resistivity was used in both theories to calculate the emissivity. The Hall coefficient was used to determine the carrier concentration. The carrier concentration was used in the FCA theory along with other parameters chosen from the literature.

The results presented herein show that the HR theory only agrees with experiment at long wavelengths and room temperature whereas the FCA theory agrees at all wavelengths and temperatures investigated.

SYMBOLS

e	electron or hole charge, 1.6×10^{-19} coulomb
k_λ	spectral absorption index
m	mass of electron, 9.11×10^{-31} kg
m^*	effective mass of electron or hole, kg
m_n^*	effective mass of electron, kg
m_p^*	effective mass of hole, kg
N	carrier concentration, cm^{-3}
N_n	electron carrier concentration, electrons/cm^3
N_p	hole carrier concentration, holes/cm^3
n_λ	spectral index of refraction
R_H	Hall coefficient, cm^3/coulomb
r_λ	normal spectral reflectivity
α_λ	spectral absorption coefficient, cm^{-1}
ϵ_λ	normal spectral emissivity
$\epsilon_{\lambda, exp}$	experimental normal spectral emissivity
$\epsilon_{\lambda, max}$	maximum values of normal spectral emissivity
ϵ_o	permittivity of free space, 8.85×10^{-12} coulomb^2/(newton)(m^2)
ϵ_∞	relative dielectric constant in the absence of any contribution from free charges at very high frequencies
λ	wavelength, μm
μ_n	mobility of electrons, (sec)(coulomb)/kg, m^2/(volt)(sec)
μ_p	mobility of holes, (sec)(coulomb)/kg, m^2/(volt)(sec)
ν	frequency, sec^{-1}
ρ	direct-current resistivity, ohm-cm
σ	conductivity, $(ohm\text{-}cm)^{-1}$
τ	relaxation time, sec
ω	frequency, rad/sec

APPARATUS AND PROCEDURE

Silicon Emissivity

Two types of commercially built spectrophotometer were used. A Perkin-Elmer Model 13 recording infrared spectrophotometer with an emittance-reflectance attachment was used to measure the normal spectral emissivity of specimens in air at temperatures of 882° and 1074° K. These measurements were taken over a wavelength range from 3.5 to 14.8 microns. The instrument was operated in the double beam mode with data recorded continuously on a strip-chart recorder. The procedure for obtaining this data and the accuracy of the measurements are discussed in appendix A.

A Perkin-Elmer Model 521 spectrophotometer with a specular reflectance attachment was used to measure the near normal specular reflectivity in air at 300° K and wavelengths of 2.5 to 35 microns. (The angle of incidence of the light beam was about 6°). This reflectivity was determined by comparing the energy reflected by the samples to that which was reflected by an aluminum mirror. The mirror was assumed to have a reflectivity of 100 percent. The normal spectral emissivity was calculated from the measured normal spectral reflectivity of the sample and the relation, $\epsilon_{\lambda} = 1 - r_{\lambda}$.

Sample Preparation for Emissivity Measurements

Ingots of single-crystal silicon were doped with arsenic to achieve electron carrier concentrations of 2.2×10^{19}, 3.7×10^{19}, and 8.5×10^{19} electrons per cubic centimeter and were doped with boron to achieve hole carrier concentrations 6.2×10^{19} and 1.4×10^{20} holes per cubic centimeter. Disks, 23 millimeters in diameter and 1.6 millimeters thick, were cut from the ingots. The front side of the samples was optically polished and was etched. Observations of the polished surface with an electron microscope showed that the width of ridges produced from the polishing procedures was about one-half micron. Two Chromel-Alumel thermocouples fabricated from 0.13-millimeter wire were mounted in a small groove sandblasted into the back side of each sample. The thermocouple junctions were spotwelded to the silicon. The thermocouple wires were held in the groove with a high-temperature cement.

Transmittance measurements were performed on samples that were optically polished on both surfaces. The measurements established that the samples were opaque at wavelengths of 2.5 to 35 microns and at a thickness of 1.6 millimeters.

Resistivity and Carrier Concentration

The values of carrier concentration $N = 1/R_H e$ and resistivity were obtained for the silicon samples with conventional Hall and direct-current resistivity apparatus and procedures. These procedures are presented in appendix B. The values of resistivity obtained herein agreed within 5 percent of the data supplied by the manufacturer. An error analysis of the Hall and the resistivity apparatus indicated that the measurements of carrier concentration and resistivity are accurate to 1 percent.

RESULTS AND DISCUSSION

Variation of Direct-Current Resistivity with Temperature

The general variation of the resistivity of doped silicon with temperature is shown in the insert of figure 1. As the temperature rises, the resistivity decreases at low temperatures (region I), increases at moderate temperatures (region II), and again decreases at the high temperatures (region III).

This investigation was performed in region II where the silicon resistivity increases as the temperature rises. Figure 1 shows the variation of resistivity with temperature (from 300° to 1200° K) and carrier concentration for both the n- and p-type semiconductors. The rising resistivity with increasing temperature is attributed to a decreasing mobility of charge carriers (ref. 3). This concept is visualized from equations

$$\rho = (N_n e \mu_n)^{-1} = (N_p e \mu_p)^{-1}$$

where the subscripts n and p refer to electrons and holes, respectively, and μ is the mobility. The carrier concentration in these heavily doped semiconductors is a constant with temperature over the range of 300° to 1100° K (ref. 3). Therefore, as ρ increases, μ_n or μ_p decreases.

Reference 3 presents extensive data on the variation of resistivity with temperature for highly doped n- and p-type silicon. Whenever it was possible, a comparison was made between the experimental resistivity obtained herein and the data of reference 3. The comparison showed agreement within ±3 percent.

Comparison of Hagen-Rubens Theory with Experiment

The experimental normal spectral emissivity of the three n-type and the two p-type

silicon specimens at temperatures of 300°, 882°, and 1074° K are shown in figures 2 and 3. As mentioned previously, the carrier concentration does not vary within this range of temperature and thus is a constant for each figure. Included in these figures is the variation of normal spectral emissivity with wavelength and temperature as interpreted by the Hagen-Rubens theory which is based on the direct-current resistivity. The equation for emissivity derived from the HR theory and the Kirchoff law is given for opaque solids as (ref. 1)

$$\epsilon_\lambda = 1 - \left\{ \frac{2\left[\frac{(\sigma)(9\times10^{11})}{\nu}\right] + 1 - 2\sqrt{\frac{(\sigma)(9\times10^{11})}{\nu}}}{2\left[\frac{(\sigma)(9\times10^{11})}{\nu}\right] + 1 + 2\sqrt{\frac{(\sigma)(9\times10^{11})}{\nu}}} \right\} \tag{1}$$

where $\sigma = 1/\rho$ and ν is the frequency of the light corresponding to the wavelength λ. The resistivity data shown in figure 1 were used to calculate the Hagen-Rubens emissivity from equation (1) at the appropriate wavelength. Figures 2 and 3 show that the best agreement of experiment and theory was achieved at the highest values of N_n or N_p in the wavelength region of 12 to 35 microns and at room temperature. As N_n or N_p decreases, the agreement at room temperature is good only at progressively greater wavelengths.

The calculated emissivity does not agree with the data taken from 3.5 to 14.8 microns and at elevated temperatures. However, the curves may asymptotically approach the calculated values at the longer wavelengths (fig. 2(a)).

Comparison of Free Carrier Absorption Theory with Experiment

Free carrier absorption theory. - The inherent assumption that causes the HR theory to break down at short wavelengths for metals and presumably for semiconductors is that the period of the light is large as compared with the relaxation time (ref. 1). A more general theory which does not make this assumption and which therefore can predict the experimental emissivity of silicon over a wider range of wavelengths is known as the free carrier absorption theory (FCA) (ref. 2). This theory predicts the emissivity in terms of the index of refraction n_λ and the absorption index k_λ.

For an opaque polished solid, the normal spectral emissivity is given from the Kirchoff law and the Fresnel formulas as

$$\epsilon_\lambda = \frac{4n_\lambda}{(n_\lambda + 1)^2 + k_\lambda^2} \tag{2}$$

Values of n_λ and k_λ can be related through the FCA theory to known or measurable quantities by the following equations:

$$\left.\begin{aligned} n_\lambda^2 - k_\lambda^2 &= \epsilon_\infty - \frac{Ne^2}{m^*\epsilon_o}\left(\frac{\tau^2}{1 + \omega^2\tau^2}\right) \\ n_\lambda k_\lambda &= \frac{Ne^2}{2\omega m^*\epsilon_o}\left(\frac{\tau}{1 + \omega^2\tau^2}\right) \end{aligned}\right\} \tag{3}$$

where e is the electron or hole charge, m* is the effective mass of electrons or holes, N is the carrier concentration of electrons or holes, ϵ_o is the permittivity of free space, ϵ_∞ is the relative dielectric constant in the absence of any contribution from free charges at very high frequencies, λ is the wavelength, and τ is the relaxation time.

Sources of values of parameters. - The physical constants e and ϵ_o are known very accurately. The carrier concentration N was determined from the experimental Hall measurements mentioned previously.

The free electron effective mass m_n^* was taken from reference 4 as 0.27, 0.26, and 0.28 m for $N_n = 2.2\times10^{19}$, 3.7×10^{19}, and 8.5×10^{19} electrons per cubic centimeter, respectively. These values were obtained from reflectivity measurements (presumably obtained at room temperature) which were then used to calculate m_n^* from equations similar to equation (3) and an $\epsilon_\infty = 11.7$. It is also shown in reference 4 that an $m_n^* = 0.26$ may be calculated from cyclotron resonance experiments. Also, an $m_n^* = 0.29$ m may be obtained from the diamagnetic susceptibility of the free carriers (ref. 4). Thus, varying types of experiments produce values of m_n^* which agree well. However, values of $m_n^* = 0.43$ m to 0.44 m for $N_n = 6.4\times10^{19}$ to 1.1×10^{20} electrons per cubic centimeter have also been published (ref. 4).

A value of $m_p^* = 0.40$ m was used in this investigation for the hole effective mass. Spitzer and Fan (ref. 5) determined $m_p^* = 0.37$ m from reflectivity measurements using a specimen with a hole concentration of 9.6×10^{18} holes per cubic centimeter. Reference 2 also shows that cyclotron resonance experiments produced a $m_p^* = 0.39$ m for holes.

Little is known about the variation of effective mass with temperature. Thus, m_n^* and m_p^* were not varied with temperature in these experiments.

Experimental determination of ϵ_∞ is difficult. Thus, data for the parameter are scarce. Reference 6 shows that values have been measured for silicon that vary from 11.7 to 14.6. A value of $\epsilon_\infty = 13 \pm 12$ percent spans this variation. A value of $\epsilon_\infty = 13$ was used herein. Reference 7 indicates that the variation of ϵ_∞ with temperature may be small. Cardona, Paul, and Brooks found a 2-percent increase in ϵ_∞ from about 70° to 300° K. Thus, no attempt was made to vary ϵ_∞ with temperature.

The relaxation time was calculated from the direct-current resistivity data given in figure 1, the values of m*, N, and e previously discussed, and the following equation:

$$\tau = \frac{m^*}{\rho N e^2} \tag{4}$$

Comparison of FCA theory with experiment. - All values of the parameters given on the right side of equation (3) have been established and thus the theoretical emissivity may be calculated. The variation of normal spectral emissivity with wavelength and temperature as interpreted by the FCA theory are presented in figures 4 and 5. Also included in figures 4 and 5 are the same experimental emissivity data presented in figures 2 and 3.

The variation of the theoretical emissivity from that of the experimental data obtained from the n- and p-type silicon at room temperature varies from about ±16 percent at $\epsilon_{\lambda, exp} = 0.19$ to ±5 percent at $\epsilon_{\lambda, exp} = 0.80$. This variance is the magnitude of the emissivity experimental error (see appendix A).

A divergence of experiment with the FCA theory was noted at the elevated temperatures. In general, the best agreement was obtained on the short wavelength side of the emissivity maximum $\epsilon_{\lambda, max}$. On the long wavelength side of $\epsilon_{\lambda, max}$, the theory predicts emissivity values smaller than experiment; the theoretical emissivity is lower than the experimental results by about 14 percent at most. These discrepancies are probably due to the small variations of ϵ_∞ and m* with temperature which were not considered.

Values of n_λ and k_λ. - The values of n_λ and k_λ, which were calculated with the FCA theory are presented in figures 6 and 7.

Spitzer and Fan (ref. 8) give values of the absorption coefficient, $\alpha_\lambda = 4\pi k_\lambda/\lambda$, calculated from measured values of room-temperature reflectivity and transmissivity of n- and p-type silicon doped to carrier concentrations ranging from about 10^{16} to 10^{19} electrons or holes per cubic centimeter, respectively. Their data, which were obtained only on the short wavelength side of $\epsilon_{\lambda, max}$, show that plots of log α_λ against log λ and plots of log α_λ against log N is a straight line at wavelengths greater than 5 microns.

The variation of log α_λ against log λ is shown in figure 8 as calculated with the

FCA theory at $N_n = 2.2\times10^{19}$ electrons per cubic centimeter and as calculated with the theory of reference 8 at $N_n = 1\times10^{19}$ electrons per cubic centimeter. Figure 8 shows that the values of log α_λ obtained from both theories vary linearly with log λ from 2 to 15 microns.

Limited calculations using the values of k_λ and N obtained herein at 6 microns also showed a linear variation of log α_λ against log N.

TABLE I. - VALUES OF NORMAL SPECTRAL EMISSIVITY AND RELAXATION TIME AT 14 MICRONS AND 1074° K

Electron carrier concentration, N_n, electrons/cm^3	Normal spectral emissivity, ϵ_λ	Relaxation time, τ, sec
8.5×10^{19}	0.46	0.39×10^{-14}
3.7	.62	.47
2.2	.69	.55
Hole carrier concentration, N_p, holes/cm^3	Normal spectral emissivity, ϵ_λ	Relaxation time, τ, sec
14×10^{19}	0.49	0.29×10^{-14}
6.2	.62	.39

TABLE II. - VALUES OF NORMAL SPECTRAL EMISSIVITY AND RELAXATION TIME AT 14 MICRONS AND ELECTRON CARRIER CONCENTRATION OF 8.5×10^{19} ELECTRONS PER CUBIC CENTIMETER

Temperature, °K	Normal spectral emissivity, ϵ_λ	Relaxation time, τ, sec
300	0.24	1.06×10^{-14}
1074	.46	.39

Interpretation of Results

The primary result of these experiments is that the normal spectral emissivity of heavily doped silicon heated to temperatures up to 1074° K agrees well with the FCA theory. Therefore, use of the FCA theory will predict the variations of ϵ_λ with wavelength, carrier concentration, and temperature shown in figures 4 and 5. The manner in which the use of FCA theory predicts these experimental variations will now be discussed.

Effect of wavelength on ϵ_λ. - The experimental emissivity of all silicon specimens passes through a maximum as the wavelength is varied. Calculated values of ϵ_λ using the FCA theory vary in a similar manner. This result can be interpreted as a coupling of n_λ and k_λ through equation (2).

Effect of carrier concentration on ϵ_λ. - The emissivity increases as N decreases and as τ increases at a constant temperature and at given wavelength ($\lambda \geq 12\,\mu$m). An example of this effect at 14 microns and 1074° K is shown in table I.

Effect of temperature on ϵ_λ at long wavelengths. - The emissivity increases as the temperature increases and as τ decreases at a constant N and at wavelengths much longer than those wavelengths corresponding to $\epsilon_{\lambda,\,max}$. An example of this effect at 14 microns and at $N_n = 8.5\times10^{19}$ electrons per cubic centimeter is shown in table II.

Effect of temperature on ϵ_λ at short wavelengths. - Little variation of ϵ_λ with temperature occurs at constant N and on the short wavelength side of $\epsilon_{\lambda, max}$. The low values of k_λ calculated at wavelengths less than those for $\epsilon_{\lambda, max}$ (fig. 6) contribute little to ϵ_λ. Since n_λ appears both in the numerator and the denominator of equation (2), changes in its value with temperature cause relatively little change in the values of ϵ_λ.

CONCLUDING REMARKS

Measurements were taken at 300°, 882°, and 1074° K of the normal spectral emissivity of heavily doped silicon. The silicon was doped with arsenic and boron to electron carrier concentration of 2.2×10^{19}, 3.7×10^{19}, and 8.5×10^{19} electrons per cubic centimeter and hole carrier concentration of 6.2×10^{19} and 1.4×10^{20} holes per cubic centimeter. The 300° K emissivities were determined from 2.5 to 35 microns, and the higher temperature emissivities were measured from 3.5 to 14.8 microns. The carrier concentration at 300° K was determined from Hall measurements. Also, the resistivity of the silicon was measured at temperatures from 300° to 1200° K. The carrier concentrations and resistivities were used in analytical calculations of the emissivities.

The emissivity data were compared with the Hagen-Rubens equation, which is based on the direct-current resistivity. This equation is known to predict well the emissivity of metals at long wavelengths and moderate temperatures. Measured resistivities were used to calculate this theoretical emissivity. Agreement of theory and experiment was found at wavelengths longer than 12 microns and at room temperature.

The experimental emissivities were also compared with the calculated values using the free carrier absorption theory (FCA). This theory considers spectral index of refraction n_λ and spectral absorption index k_λ to be functions of electron or hole charge e, effective mass of electron or hole m*, carrier concentration N, permittivity of free space ϵ_0, relative dielectric constant in the absence of any contribution from free charges at very high frequencies ϵ_∞, wavelength λ, and relaxation time τ. The constants e and ϵ_0 are known accurately. The relaxation time is a function of direct-current resistivity ρ, N, m*, and e. The experimental values of ρ and N determined herein were used to determine τ. The values of m* were obtained from the literature. The value of ϵ_∞, as determined by other experiments, is not known as accurately as other parameters. Thus, it was necessary to choose ϵ_∞ within the range of values given in the literature such that the theoretical variation of emissivity with wavelength could be more closely fitted to the experimental variations of normal spectral emissivity ϵ_λ.

Good agreement of the FCA theory and experiment was achieved for both p-type

and n-type silicon at all wavelengths and temperatures investigated (λ of 2.5 to 35 μm at 300° K and λ of 3.5 to 14.8 μm at 882° and 1074° K). Therefore, it was concluded that the FCA theory as applied to silicon with carrier concentration N greater than 10^{19} per cubic centimeter is a proper physical law for predicting and interpreting the experimental variations of ϵ_λ with wavelength, carrier concentration, and temperature observed in these experiments.

It was generally found that the emissivity calculated with the FCA theory (1) passed through a maximum as the wavelength varied, (2) varied little with temperature at a constant value of N and at all wavelengths corresponding to the short wavelength side of $\epsilon_{\lambda,\max}$, (3) increased as N decreased and as τ increased at a constant temperature and at wavelengths of about 12 microns or greater, and (4) increased as the temperature increased and as τ decreased at a constant N and at wavelengths much longer than those wavelengths corresponding to $\epsilon_{\lambda,\max}$.

The index of refraction n_λ and the absorption index k_λ of the silicon specimens at temperatures of 300°, 882°, and 1074° K were also obtained with the FCA theory. The values of k_λ obtained from the FCA theory at 300° K were used to calculate the spectral absorption coefficient α_λ. These values of α_λ were compared with those in the literature that are based on the optical ray absorption theory (ref. 8). Good qualitative agreement was obtained from this comparison. Thus, it was concluded that the FCA theory can be used with reasonable accuracy to obtain the n_λ and k_λ of opaque media. Also, it is expected that high-temperature optical properties of highly doped germanium, cadmium sulfide, and alloys of silicon and germanium may also be obtained from the free carrier absorption theory.

Lewis Research Center,
National Aeronautics and Space Administration,
Cleveland, Ohio, March 16, 1967,
120-27-01-20-22.

APPENDIX A

PROCEDURE FOR OBTAINING EMISSIVITY DATA AND ACCURACY OF MEASUREMENTS

The uncertainty associated with the type of emissivity measurements made herein has been discussed by many authors. A good discussion covering most of the possible errors is given in reference 9. One such error arises from a mismatch between the specimen temperature and the hohlraum temperature. The difference can arise because the thermocouples are not recording the true specimen temperature and because of intolerable temperature gradients in the hohlraum. The following discussion will show how the errors were minimized in these experiments.

Emittance of Standard

Alumina (Al_2O_3), flame sprayed to a thickness of 0.4 millimeter on a roughened stainless steel substrate, was used as a standard to achieve a temperature match for this system. Thermocouples were added to the substrate in the manner previously discussed for silicon. The results of experiments by others measuring normal spectral emittance or reflectance agree that Al_2O_3 either in powdered, flame-sprayed, or sintered form has an emittance of 0.95 to 0.99 at 8.5 microns over a range of temperatures from about 300° to 1300° K and over a wide range of surface roughness and thickness. A spectral emittance of the standard of 0.97 to 0.99 at 8.5 microns was achieved with the hohlraum and standard temperature settings given in table III. (The hohlraum has an advertized emittance of 0.99). The lower indicated standard temperatures as compared to the hohlraum temperatures are attributed to heat conduction through the thermocouples and a measured temperature gradient through the standard of 2° at about 880° K and 4° at about 1070° K. The hohlraum used in these experiments possessed a temperature gradient of 8° at about 890° K and 15° at about 1090° K. These small temperature gradients were achieved by inserting a ceramic plug into the hole in the hohlraum normally occupied by the reflectance sample holder.

Figure 9 shows the normal spectral emittance of the standard from about 1.2 to 14.8 microns at the temperature settings given in table III and also at 300° K. The reflectivity attachment on the Perkin-Elmer Model 13 spectrophotometer was used to obtain the room-temperature emittance. The good agreement of the data from about 1 to 2.5 microns and from about 4 to 14.8 microns indicates that a reasonable temperature match between hohlraum and standard has been established.

TABLE III. - STANDARD AND HOHLRAUM TEMPERATURE SETTINGS NECESSARY TO ACHIEVE NORMAL SPECTRAL EMISSIVITY OF 0.97±0.03 AT 8.5 MICRONS

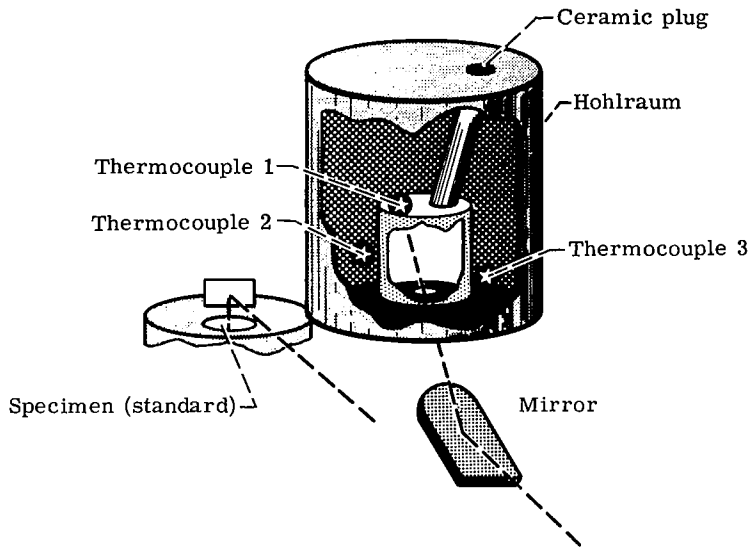

Thermocouple			Average temperature, ^{o}K	Standard temperature settings, ^{o}K
1	2	3		
Hohlraum temperature setting, ^{o}K				
891	894	886	882	874 873 872
1088	1095	1080	1074	1058 1060 1061

The room-temperature data shown in figure 9 were found to agree well with room-temperature measurements on flame-sprayed alumina (ref. 10). This agreement included complete verification of the emittance peak shown at about 3 microns (fig. 9). This peak is generally considered to be caused by absorbed water. Thus, the variations of ϵ_{λ} with temperature at wavelengths of about 2.5 to 4 microns are probably caused by more absorbed water present in the alumina at 300^{o} K than at 1074^{o} K.

High-Temperature Emissivity of Silicon

The temperature settings given in table III as obtained with the alumina standard

were used to obtain the normal spectral emissivity of the various silicon samples. However, good emissivity data may be obtained from the silicon specimens by using the standard as reference only if the surface temperatures are about equivalent and the heat conduction loss along the thermocouple wires is about the same for both materials.

The temperature gradient across a silicon specimen with $N_n = 2.2 \times 10^{19}$ electrons per cubic centimeter was experimentally found to be 3° at about 880° K and 5° at about 1070° K. Thus, the temperature drop across the silicon and the standard are within 1° K.

The heat loss through the thermocouple wires could not be determined experimentally, and therefore a rough estimate of this loss was made analytically. Theory (ref. 11) shows that the thermocouple wires attached to the standard and the silicon may indicate different (and low) temperatures even though the specimens may, in fact, be at identical temperatures. The reason for this is that the heat conducted to the thermocouple wires welded to the stainless steel (standard) can be different from that conducted along the wires welded to the silicon. However, it was calculated that there was an identical heat loss along the thermocouple wires attached to either the silicon or the stainless steel.

From the theory of reference 11, the thermocouples were calculated to read about 20° K lower than the true specimen temperature at temperatures of 900° to 1100° K. This error is very close to that shown in table III.

The silicon surface is known to oxidize when exposed to air and this oxidation is more rapid at high temperatures. The oxidation, if sufficiently rapid, could cause large inaccuracies in the emissivity data. To evaluate the effect of oxidation on emissivity, measurements were made of the room-temperature emissivity before and after the emissivity was measured in air at the elevated temperatures. Negligible variations of the room-temperature emissivity were observed.

The previous discussion has indicated that the experimental error associated with the high-temperature silicon emissivity is small. This experimental error is considered to be between ±4 and 7 percent.

The hohlraum and standard temperatures were averaged to obtain the average temperature given in table III. These average temperatures are 882° and 1074° K. All the silicon properties needed to establish the correspondence between theory and experiment were evaluated at these two average temperatures and at room temperature (300° K).

Room-Temperature Reflectivity

The room-temperature, specular, near normal reflectivity of all the silicon specimens was measured at wavelengths of 2.5 to 35 microns. For comparison, the total

(specular plus diffuse) reflectivity of the silicon from 3.5 to 14.8 microns was also measured using the reflectivity-attachment on the Perkin-Elmer Model 13 spectrophotometer. The specular and total reflectivity measurements generally were found to vary from ±16 percent at a specular $\epsilon_\lambda = 0.19$ to ±5 percent at a specular $\epsilon_\lambda = 0.80$. Therefore, the room-temperature specular reflectivity is believed to be accurate at least to these percentages.

Howarth and Gilbert (ref. 4) experimentally determined the room temperature spectral reflectivity of highly doped n-type silicon for purposes of determining the free electron effective mass. A comparison of their data obtained at wavelengths of 3.5 to 14.8 microns with the data obtained herein indicated good agreement.

APPENDIX B

HALL EFFECT AND RESISTIVITY MEASUREMENTS

Room-temperature Hall measurements and resistivity measurements at both room and elevated temperatures were obtained on conventional four-ear bridge-shaped specimens with an automated Hall effect and resistivity facility. Since the sample suspension system for this apparatus was designed primarily for use between 4.2° and 400° K, a special high-temperature resistivity sample mount was fabricated for use up to approximately 1200° K (fig. 10).

The samples were cut from silicon wafers using air abrasive techniques and generally measured approximately 1.3×10^{-2} meter in length by 1.5×10^{-3} meter in width. The sample thickness varied between the limits of 5.4×10^{-4} and 1.04×10^{-3} meter. Ohmic contacts were obtained through use of various solders and spark-welding techniques. The ohmic contacts were verified and frequently monitored during measurements with curve tracing equipment that displays diode characteristics.

In determining the Hall coefficient R_H and resistivity ρ, techniques were used which eliminated errors arising from the various thermoelectric and thermomagnetic effects that influence the apparent Hall or resistivity voltages. A detailed discussion of these problems and procedures to eliminate them have been published by Harman (ref. 12).

The Hall coefficient R_H was calculated from the expression

$$R_H = \frac{\langle V_H \rangle \times t \times 10^{10}}{IH}$$

where

R_H Hall coefficient, cm^3/coulomb

$\langle V_H \rangle$ algebraic average of four Hall voltages measured under both forward and reverse polarity conditions of both sample current and magnetic field, V

I sample current, A

H magnetic field strength, Wb/m^2

t sample thickness m

The carrier concentration N is then calculated from the expression

$$N = \left| \frac{1}{R_H e} \right|$$

where

e electronic charge = 1.6021×10^{19} coulomb

N carrier concentration, cm^{-3}

The electric resistivity ρ was calculated from the expression

$$\rho = \frac{V_R}{I} \times \frac{a}{l} \times 10^2$$

where

ρ resistivity, (ohm)(cm)

V_R voltage measured between resistivity probes, V

a product of sample width and thickness, m^2

l spacing between resistivity probes, m

Room-Temperature Hall and Resistivity Measurements

The following techniques were used to obtain ohmic contacts. Indium was soldered to the n-type arsenic-doped sample with N equal 2.2×10^{19} electrons per cubic centimeter. Pressure probes were then spark welded to the indium. For the samples with N values equal to 8.5×10^{19} electrons per cubic centimeter and 3.7×10^{19} electrons per cubic centimeter, 50-percent-lead and 50-percent-tin solder was used as the contact material to the silicon. The pressure probes were then spark welded to the solder. For the two boron-doped p-type silicon samples, ohmic contacts were formed by spark welding aluminum foil discs to the silicon and by making pressure probe contacts with the aluminum.

Sample temperatures were measured by attaching copper-constantan thermocouples to the specimens with varnish.

Resistivity Measurements at Elevated Temperatures

The sample mount used for the resistivity work at elevated temperatures is shown in figure 10. The mount construction consisted of a boron nitride mounting base, a stainless-steel suspension tube, a stainless-steel mounting hardware, ceramic insula-

tors, and 92-percent-platinum - 8-percent-tungsten probes and lead wires with a diameter of 0.013 centimeter. Also shown in figure 10 is a bridge-shaped sample of silicon mounted for measurement, with its six electric leads attached. The Chromel-Alumel thermocouple used for all the elevated temperature determinations is shown spark welded to the sample and held in place with a pressure arm. The sample holder was heated in a quartz tube which extended through a 1-inch-tube furnace. An argon atmosphere was maintained in the tube during heating with a flow rate of approximately 0.5 cubic centimeter per minute.

Ohmic contacts were obtained on the arsenic-doped n-type samples by spark-welding the platinum-tungsten wire directly to the silicon. For the boron-doped p-type material, aluminum foil discs were sandwiched between the probe wires and the silicon. The aluminum foil, probe wires, and silicon were then spark welded to form the contact.

The room temperature resistivity was remeasured following some of the elevated temperature runs and was found to agree with the initial values.

REFERENCES

1. Born, Max; and Wolf, Emil: Principles of Optics; Electromagnetic Theory of Propagation, Interference and Diffraction of Light. Second ed. Pergamon Press, 1964.

2. Moss, Trevor S.: Optical Properties of Semi-Conductors. Academic Press, 1959.

3. Chapman, P. W.; Tufte, O. N.; Zook, J. David; and Long, Donald: Electrical Properties of Heavily Doped Silicon. J. Appl. Phys., vol. 34, no. 11, Nov. 1963, pp. 3291-3295.

4. Howarth, L. E.; and Gilbert, J. F.: Determination of Free Electron Effective Mass on n-Type Silicon. J. Appl. Phys., vol. 34, no. 1, Jan. 1963, pp. 236-237.

5. Spitzer, W. G.; and Fan, H. Y.: Determination of Optical Constants and Carrier Effective Mass of Semiconductors. Phys. Rev., vol. 106, no. 5, June 1, 1957, pp. 882-890.

6. Runyan, W. R.: Silicon Semiconductor Technology. McGraw Hill Book Co. Inc., 1965.

7. Cardona, M.; Paul, W.; and Brooks, H.: Dielectric Constant Measurements in Germanium and Silicon at Radio Frequencies as a Function of Temperature and Pressure. Semiconductors. Vol. 1, pt. 1 of Solid State Physics in Electronics and Telecommunications. M. Désirant and J. L. Michiels, eds., Academic Press, 1960, pp. 206-214.

8. Spitzer, W.; and Fan, H. Y.: Infrared Absorption in n-Type Silicon. Phys. Rev., vol. 108, no. 2, Oct. 15, 1957, pp. 268-271.

9. Streed, E. R.; McKellar, L. A.; Rolling, R., Jr.; and Smith, C. A.: Errors Associated with Hohlraum Radiation Characteristics Determinations. Measurement of Thermal Radiation Properties of Solids. Joseph C. Richmond, ed. NASA SP-31, 1963, pp. 237-252.

10. Liebert, Curt H.: Spectral Emittance of Aluminum Oxide and Zinc Oxide on Opaque Substrates. NASA TN D-3115, 1965.

11. Chapman, Alan J.: Heat Transfer. MacMillian Co., 1960.

12. Herman, T. C.: Measurement of Pertinent Thermoelectric Properties. Thermoelectric Materials and Devices. Irving B. Cadoff and Edward Miller, eds., Reinhold Publishing Corp., 1960, pp. 84-97.

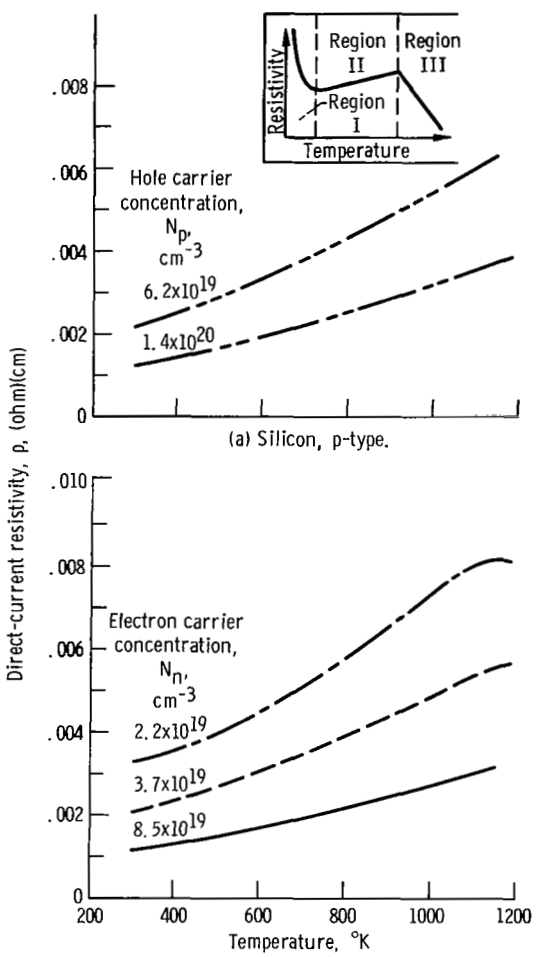

(a) Silicon, p-type.

(b) Silicon, n-type.

Figure 1. - Direct-current resistivity of n- and p-type silicon.

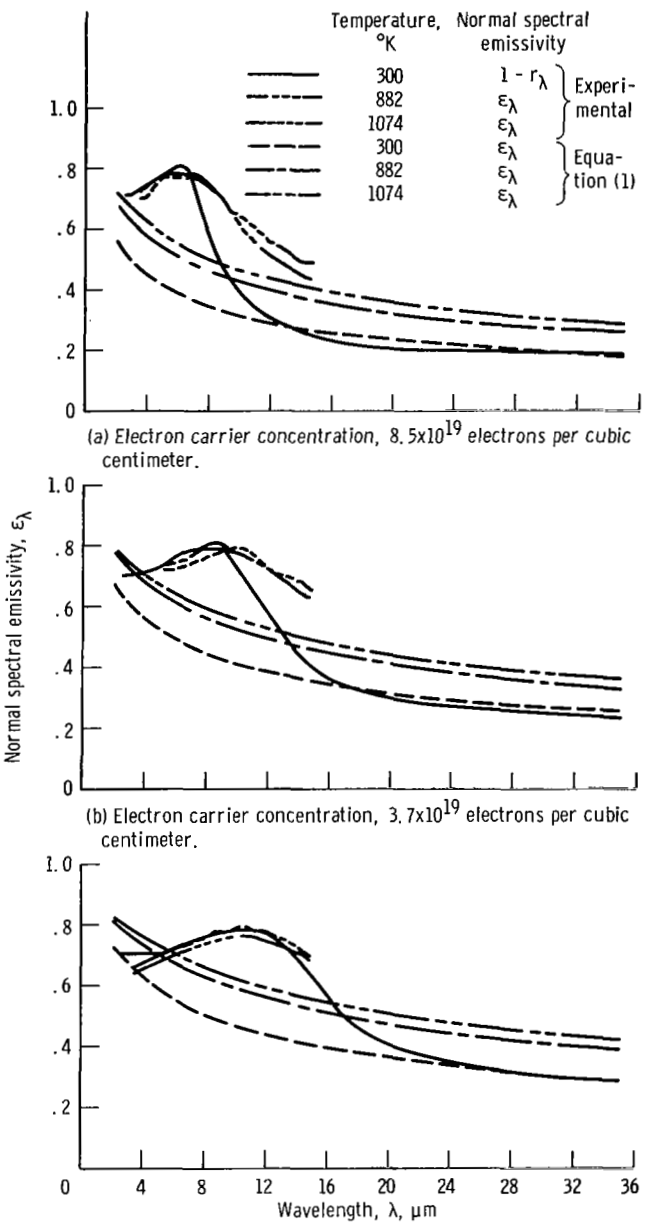

(a) Electron carrier concentration, 8.5×10^{19} electrons per cubic centimeter.

(b) Electron carrier concentration, 3.7×10^{19} electrons per cubic centimeter.

(c) Electron carrier concentration, 2.2×10^{19} electrons per cubic centimeter.

Figure 2. - Comparison of HR theory with experiment.

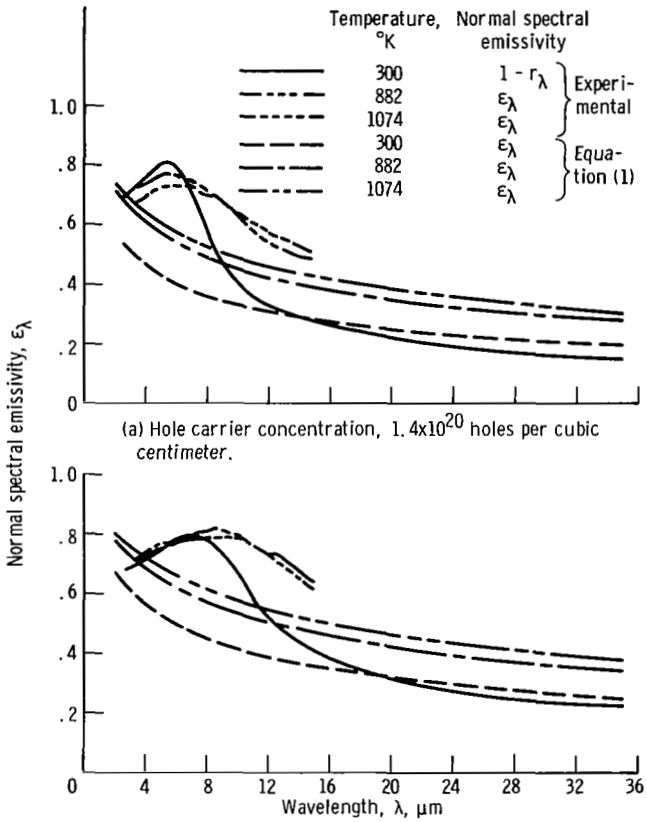

(a) Hole carrier concentration, 1.4×10^{20} holes per cubic centimeter.

(b) Hole carrier concentration, 6.2×10^{19} holes per cubic centimeter.

Figure 3. - Comparison of HR theory with experiment.

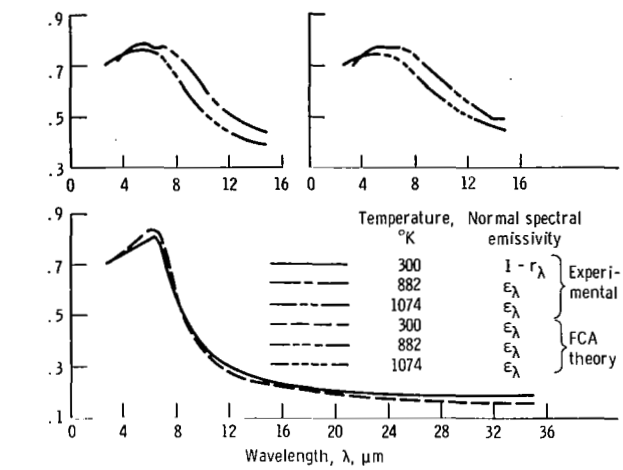

(a) Electron carrier concentration, 8.5×10^{19} electrons per cubic centimeter.

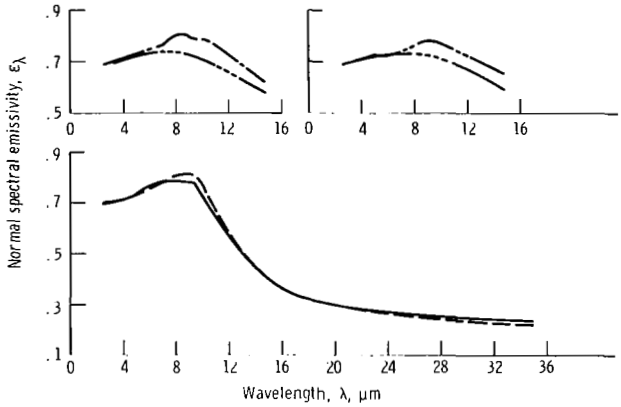

(b) Electron carrier concentration, 3.7×10^{19} electrons per cubic centimeter.

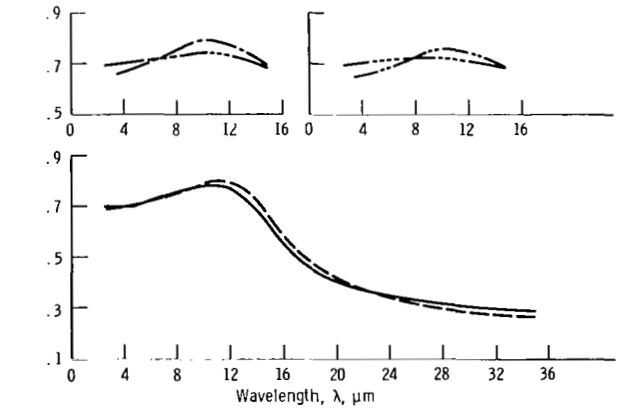

(c) Electron carrier concentration, 2.2×10^{19} electrons per cubic centimeter.

Figure 4. - Comparison of FCA theory with experiment.

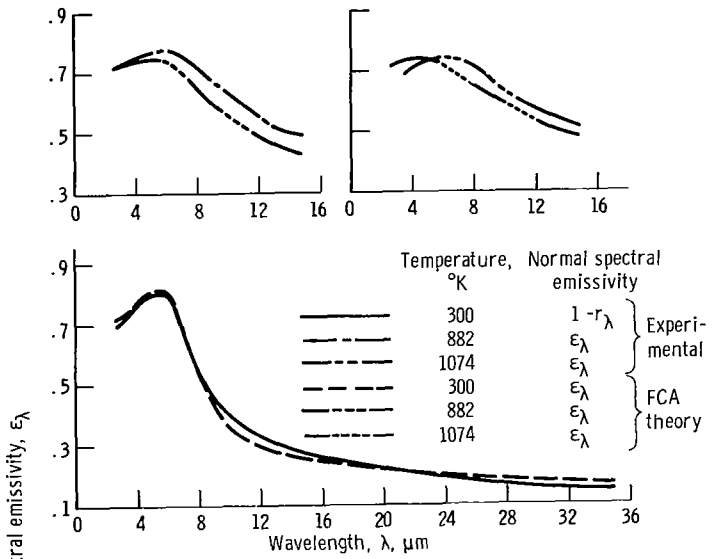

(a) Hole carrier concentration, 1.4×10^{20} holes per cubic centimeter.

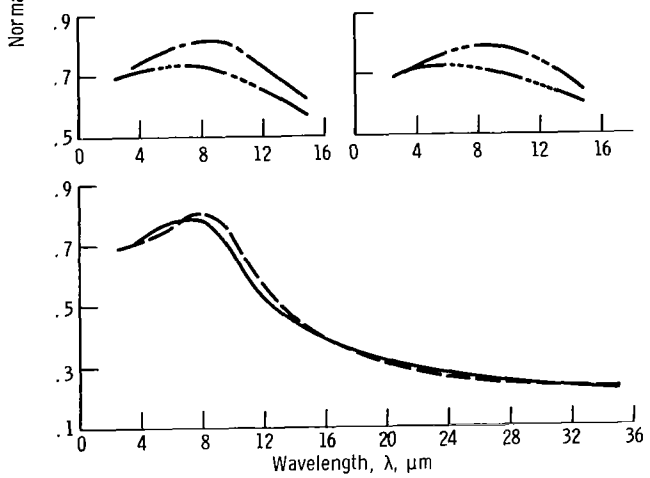

(b) Hole carrier concentration, 6.2×10^{19} holes per cubic centimeter.

Figure 5. - Comparison of FCA theory with experiment.

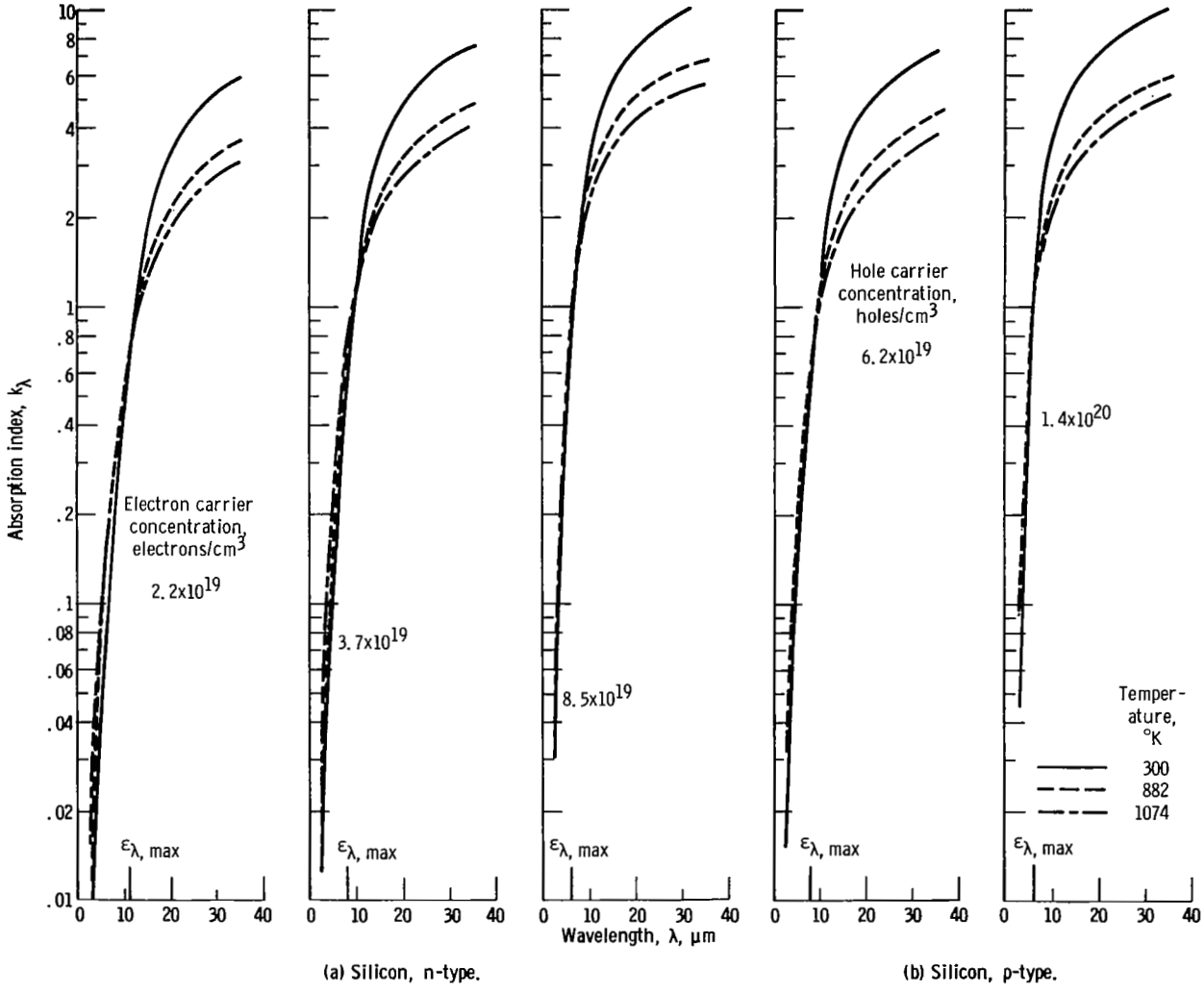

Figure 6. - Spectral absorption index of highly doped silicon.

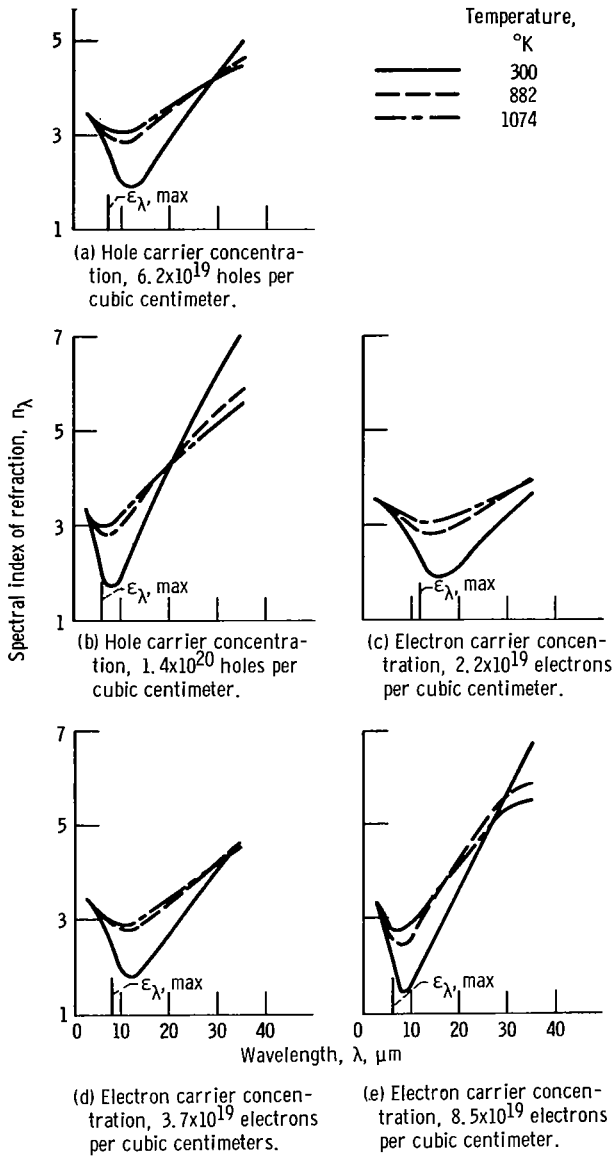

(a) Hole carrier concentration, 6.2×10^{19} holes per cubic centimeter.

(b) Hole carrier concentration, 1.4×10^{20} holes per cubic centimeter.

(c) Electron carrier concentration, 2.2×10^{19} electrons per cubic centimeter.

(d) Electron carrier concentration, 3.7×10^{19} electrons per cubic centimeters.

(e) Electron carrier concentration, 8.5×10^{19} electrons per cubic centimeter.

Figure 7. - Index of refraction of n- and p-type silicon.

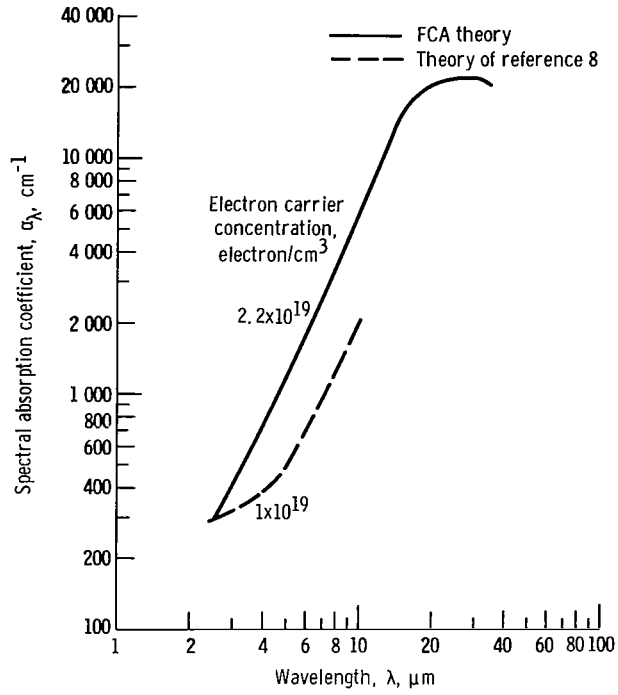

Figure 8. - Comparison of room temperature absorption coefficients obtained with FCA and reference 8 theories.

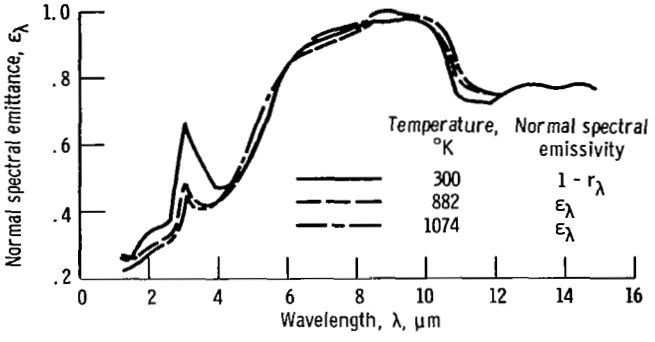

Figure 9. - Spectral emittance of flame-sprayed alumina standard.

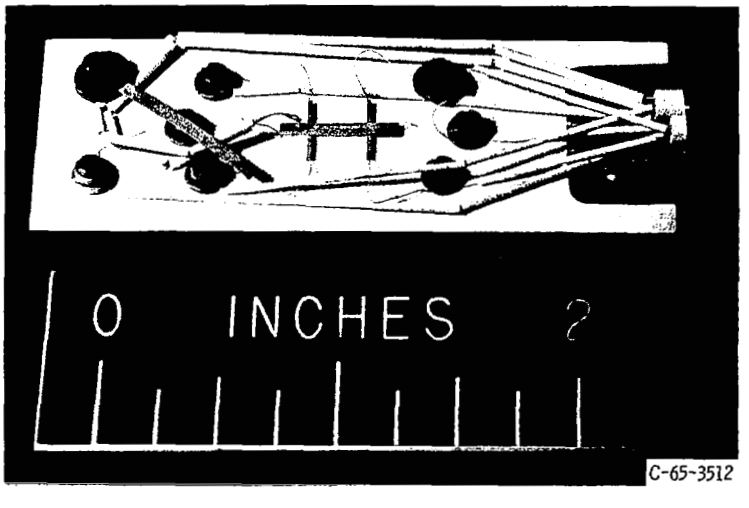

Figure 10. - High-temperature resistivity sample mount.